ORIGINAL ARTICLE

Episodic Aspiration with Oral Commensals Induces a MyD88-dependent, Pulmonary T-Helper Cell Type 17 Response that Mitigates Susceptibility to *Streptococcus pneumoniae*

Benjamin G. Wu[1,2,3], Imran Sulaiman[1,3], Jun-Chieh J. Tsay[1,2,3], Luisanny Perez[1,3], Brendan Franca[1,3], Yonghua Li[1,3], Jing Wang[1,4], Amber N. Gonzalez[1,3], Mariam El-Ashmawy[3], Joseph Carpenito[1,3], Evan Olsen[1,3], Maya Sauthoff[1,3], Kevin Yie[1,3], Xiuxiu Liu[5], Nan Shen[6], Jose C. Clemente[6], Bianca Kapoor[3], Tonia Zangari[7], Valeria Mezzano[8,9], Cynthia Loomis[9,10], Michael D. Weiden[1,3], Sergei B. Koralov[10], Jeanine D'Armiento[11], Sunil K. Ahuja[12], Xue-Ru Wu[10,13], Jeffrey N. Weiser[7], and Leopoldo N. Segal[1,3]

[1]Division of Pulmonary, Critical Care and Sleep Medicine, [3]Department of Medicine, [9]Division of Cardiology, Department of Medicine and [10]Department of Pathology, NYU Langone Health, New York, New York; [7]Department of Microbiology, [8]Experimental Pathology Research Laboratory, Division of Advanced Research Technologies, and [13]Department of Urology, School of Medicine, New York University, New York, New York; [2]Division of Pulmonary and Critical Care, New York Harbor Veterans Affairs, New York, New York; [4]Beijing Chaoyang Hospital, Capital Medical University, Beijing, China; [5]Division of Pediatrics, Longhua Hospital, Shanghai University of Chinese Medicine, Shanghai, China; [6]Department of Genetics and Genomic Sciences and Immunology Institute, Icahn School of Medicine at Mount Sinai, New York, New York; [11]Department of Anesthesiology, School of Medicine, Columbia University, New York, New York; and [12]University of Texas Health Science Center, San Antonio, Texas

ORCID ID: 0000-0001-8547-5678 (B.G.W.).

Abstract

Rationale: Cross-sectional human data suggest that enrichment of oral anaerobic bacteria in the lung is associated with an increased T-helper cell type 17 (Th17) inflammatory phenotype.

Objectives: In this study, we evaluated the microbial and host immune-response dynamics after aspiration with oral commensals using a preclinical mouse model.

Methods: Aspiration with a mixture of human oral commensals (MOC; *Prevotella melaninogenica*, *Veillonella parvula*, and *Streptococcus mitis*) was modeled in mice followed by variable time of killing. The genetic backgrounds of mice included wild-type, MyD88-knockout, and STAT3C backgrounds.

Measurements and Main Results: 16S-rRNA gene sequencing characterized changes in microbiota. Flow cytometry, cytokine measurement via Luminex and RNA host-transcriptome sequencing was used to characterize the host immune phenotype. Although MOC aspiration correlated with lower-airway dysbiosis that resolved within 5 days, it induced an extended inflammatory response associated with IL-17–producing T cells lasting at least 14 days. MyD88 expression was required for the IL-17 response to MOC aspiration, but not for T-cell activation or IFN-γ expression. MOC aspiration before a respiratory challenge with *S. pneumoniae* led to a decrease in hosts' susceptibility to this pathogen.

Conclusions: Thus, in otherwise healthy mice, a single aspiration event with oral commensals is rapidly cleared from the lower airways but induces a prolonged Th17 response that secondarily decreases susceptibility to *S. pneumoniae*. Translationally, these data implicate an immunoprotective role of episodic microaspiration of oral microbes in the regulation of the lung immune phenotype and mitigation of host susceptibility to infection with lower-airway pathogens.

Keywords: microbiome; inflammation; transcriptomics; pathogen susceptibility

At a Glance Commentary

Scientific Knowledge on the Subject: Enrichment of the lower-airway microbiota with oral commensals has been observed in human cross-sectional studies in both health and disease and is associated with host immune tone. However, the potential mechanisms for this association are not known. Therefore, we took an experimental approach using a preclinical model of aspiration with oral commensals to evaluate its implication on host immune tone and susceptibility to pathogens.

What This Study Adds to the Field: A single episode of aspiration of human oral commensals (*Streptococcus mitis, Veillonella parvula,* and *Prevotella melaninogenica*) leads to transient lower-airway dysbiosis but leads to a prolonged increase in lower-airway inflammatory tone and to a decrease in the susceptibility to a pathogen (*S. pneumoniae*). These data provide a framework to understand how the most common microbial exposure in the lower airways affects lung immunity and susceptibility to respiratory pathogens.

Microaspiration of oral commensals is a common and nearly daily occurrence. Supporting this observation, in otherwise healthy persons, lower-airway microbiota harbor a complex microbial community frequently enriched with human oral commensals (1–3). Given that the upper and lower airways comprise a contiguous anatomic system, transient aspiration of upper airway microbiota into the lower airways is likely a physiological phenomenon and may even impart a protective immunological phenotype to the lower airways. In contrast, chronic inflammatory airway conditions, such as

asthma (4, 5), lung transplant (6), and chronic obstructive pulmonary disease (7–11) may associate with lower-airway dysbiosis where oral commensals are frequently observed. The latter dysbiotic signature is often associated with increased IL-17 inflammation (4, 12), and in a murine model of asthma, IL-17 induction appeared to be dependent on MyD88-linked innate immunity (13).

On the basis of these observations, in a murine model, we tested the hypothesis that a single aspiration with a mixture of human oral commensals (MOC) induces a T-helper cell type 17 (Th17) response in the lower airway. Th17 induction is dependent on a MyD88-associated innate immune mechanism and modifies susceptibility to *Streptococcus pneumoniae*, a common respiratory pathogen. Our results support these hypotheses. MOC aspiration protected mice against *S. pneumoniae*–associated infection and mortality. Collectively, these findings raise the provocative possibility that episodic oral commensal microaspiration may confer an immunological benefit linked to a transient increase in the Th17-associated inflammatory pathway.

Methods

Ethics Statement

The animal studies described in these experiments were approved by the Institutional Animal Care and Use Committee at the respective institutions (New York University School of Medicine Institutional Animal Care and Use Committee number s16-00032). Laboratory animal care policies follow the Public Health Service Policy on Humane Care and Use of Laboratory Animals.

Animals: Mice

Female C57BL/6J mice (8–14 wk of age, 18–22 g/mouse) were purchased from Jackson Research Laboratories (catalog number [Cat#] 000664). MyD88-knockout (MyD88KO) mice were purchased from

Jackson Research Laboratories (Cat# 009088). In addition, we used a mouse model with hyperactive STAT3 selectively expressed in T lymphocytes, leading to a pronounced Th17 bias and IL-17–mediated lung pathology (14). For further details, *see* the online supplement.

Microorganisms: Bacteria

Human oral commensals. The following human oral commensals were obtained: *Veillonella parvula* (17742; American Type Culture Collection [ATCC]), *Prevotella melaninogenica* (25845; ATCC), and *S. mitis* (49456; ATCC). These bacteria were grown in anaerobic conditions (Bactron 300; Shel Labs) and then stored in 20% glycerol tryptic soy broth at $-80°C$. To prepare the oral commensal challenges, the bacterial strains were thawed and streaked on prereduced anaerobically sterilized *Brucella* Blood agar plates (Anaerobe Systems). For each experimental comparison, the same MOC was used. The microbial aliquots (50 μl) used for intratracheal challenge will be referred to as an MOC (consisting of *Streptococcus*, *Veillonella*, and *Prevotella*). This combination of oral commensals was chosen on the basis of the composition of prior human-lung microbiome work (3, 12). Further details can be found in the online supplement.

Human pathogen challenge. To evaluate host susceptibility to pathogens, we used a P1397 strain of *S. pneumoniae*. A low concentration of *S. pneumoniae* is defined as $1–7.9 \times 10^8$ cfu/ml, a medium concentration of *S. pneumoniae* is defined as $8 \times 10^8–1.9 \times 10^9$ cfu/ml, and a high concentration of *S. pneumoniae* is defined as $>2 \times 10^9$ cfu/ml. Experiments that were performed for the recovery of *S. pneumoniae* used 1×10^8– to 3×10^9–cfu/ml concentrations. Recovery of *S. pneumoniae* was evaluated in lung lavage 24 hours after challenge by culturing on tryptic soy agar with streptomycin plates.

Further details can be found in the online supplement.

Intratracheal microbial challenges. A detailed description of intratracheal microbial challenges can be found in the online supplement.

Measurements

Fluorescence-activated cell sorter analysis. Fluorescence-activated cell sorter (FACS) analysis was performed on a single-cell suspension derived from lung homogenate. The cells were surface stained, fixed in 2% paraformaldehyde, and permeabilized with 0.5% saponin. Fluorochrome-conjugated antibodies with the following specificities were used: $CD3^+$ (BD Bioscience); $TCR\beta^+$, $TCR\gamma\delta^+$, $CD4^+$, $CD8^+$, $CD69^+$, $PD1^+$, $CD44^+$, $CD62L^+$, $CD25^+$, $IL17^+$, $IL10^+$, and $IL2^+$ (BioLegend); and $IFN\text{-}\gamma^+$, $IL4^+$, $FOXP3^+$, and $ROR\gamma T^+$ (*see* Table E1 [FACS table] in the online supplement; all antibodies are from Thermo Fisher Scientific unless otherwise specified). The cell-staining measurements of the samples were performed on a BD LSR II flow cytometer (BD Bioscience) and data was analyzed using FlowJo version 10.3 (v10.3) (Tree Star Inc.) (14). Further details can be found in the online supplement.

Cytokine and chemokine measurement in lung homogenate. Cytokines and chemokines were measured using Luminex (Murine Cytokine Panel II; EMD Millipore). Lung homogenates were thawed and processed according to the recommended protocol using the Murine Cytokine/Chemokine Magnetic Bead Panel (MCYTMAG-70K-PXkl32). All cytokine/chemokine concentrations were normalized by the gram of lung homogenate (15) and included those with dynamic range: G-CSF, Eotaxin, IFN-γ, IL-1α, Il-1β, IL-3, IL-4, IL-5, IL-6, IL-7, IL-9 IL-10, IL-12p40, IL-12p70, LIF, IL-17, IP-10, KC, MCP-1, MIP-1α, MIP-1β, M-CSF, MIP-2, MIG, RANTES, VEGF, and TNF-α.

Multiplex immunofluorescence staining. Five-micron sections of paraffin-embedded preserved lung tissue were stained using the Akoya Biosciences Opal multiplex automation kit (Akoya Biosciences) for six antibodies and DAPI (Table E2 [antibody table]). Semiautomated image acquisition was performed on a Vectra 3.0 imaging system (PerkinElmer).

Further details can be found in the online supplement.

Microbiome analysis and differential abundance calculation. To evaluate changes in the microbiome, we performed 16S-rRNA gene sequencing of obtained samples, including lung, nasal, oral, and gut samples. Negative controls included unused, sterile phosphate-buffered saline (PBS) samples passed through instruments and disposables used for sampling (16). In addition, DNA-free water passed through a DNA extraction kit was used as a technical control. Mock bacterial-community DNA were run during DNA sequencing for positive sequence controls. Samples from mice were stored at −80°C until DNA extraction. DNA was extracted with an ion-exchange column (Qiagen). Amplification and detection of the V4 16S rRNA gene by quantitative PCR was performed with the StepOne Real-Time PCR System (Applied Biosystems). Sequencing was then performed in MiSeq (Illumina) to produce 150 base-paired end reads (17). For all samples, we obtained >5,000 reads per sample (reads = 47,256 [37,662–55,650]).

The 16S-rRNA gene sequences were analyzed using the Quantitative Insights into Microbial Ecology (v2.0, 2019.07 release) pipeline for analysis of microbiome data (18, 19). Reads were demultiplexed and quality filtered with default parameters. After demultiplexing, sequences were matched through the Divisive Amplicon Denoising Algorithm 2 (DADA2) pipeline (19, 20) to generate representative sequences and a frequency table consisting of amplicon sequence variants (ASV) (21).

The Shannon Diversity Index on rarefied data was used to evaluate α diversity (within sample diversity). Weighted unique fraction (UniFraq) was used to measure β diversity (between-sample diversity) of bacterial communities and to perform principal coordinate analysis (PCoA) (22). We used the ade4 package in R (R Foundation for Statistical Computing) to plot a PCoA on weighted UniFrac distances (23). Further details can be found in the online supplement. Microbiome data are publicly available from the Sequence Read Archive under accession number PRJNA588801. Code and metadata used for analysis are available at https://github.com/segalmicrobiomelab/murine.host.microbiota.interaction/.

Transcriptome of lung homogenate. Flash-frozen lung samples were defrosted and then homogenized using a hand TissueRuptor II on the second lowest setting (Qiagen). RNA was extracted from collected supernatant using the Qiagen miRNeasy Mini Kit (Cat# 74135; Qiagen). Quality control was established with an RNA integrity number cutoff > 6. RNA sequencing was performed using HiSeq (Illumina) at the New York University Genomic Technology Center. Sequences from the murine lung homogenate were aligned against the murine ensemble reference genome using the Spliced Transcripts Alignment to a Reference (STAR) (v2.5) aligner (24). Gene counting of each sample was performed using featureCounts (v1.5.3) (25, 26), and gene differential expression was calculated using the DESeq2 (v3.5) package in R (v3.6) (27). Genes with an adjusted P value (false discovery rate [FDR]) $Q < 0.10$ were considered significantly differentiated, unless otherwise specified (Table E3). Ingenuity pathway analysis (IPA) was used to identify the most differential biological functions, disease/disorders, and regulator effect networks and to generate top canonical/network pathways (https://qiagenbioinformatics.com/products/ingenuity-pathways-analysis; Qiagen) (28, 29). Networks generated by IPA grouped the differentially regulated genes according to known associations between genes and proteins (28, 29). Genes were mapped to Ensembl identifiers (bioDBnet) and subsequently to Kyoto Encyclopedia of Genes and Genomes pathways (KEGG Pathway Database) and were summarized at levels 1–3. When a gene was annotated to multiple pathways, equal counts were added to each of the pathways. Further details can be found in the online supplement. Murine transcriptome data can be found under the BioProject identifier in the NIH Sequence Read Archive (PRJNA603050).

Statistical Analysis

Because the distributions of microbiome data are nonnormal, and no distribution-specific tests are available, we used nonparametric tests of association for analysis. For association with discrete factors, we used either the Mann-Whitney test (in the case of two categories) or the Kruskal-Wallis ANOVA (in case of more than two categories). For tests of association

with continuous variables, we used nonparametric Spearman (ρ) correlation tests. The FDR ($Q < 0.10$) was used to control for multiple testing in gene expression (30). For the remaining analysis for multiple comparisons, we used an FDR of $Q < 0.05$. To evaluate differences in community composition between groups on the basis of 16S data and a categorical or continuous variable, we used permutational multivariate ANOVA (PERMANOVA or Adonis) with 1,000 permutations.

Results

Longitudinal Change in Microbiota after Single MOC Aspiration
To investigate the effects of episodic aspiration events with human oral commensals *V. parvula*, *P. melaninogenica* and *S. mitis* (hereafter referred to as the MOC) on the mouse microbiota, we sampled the lung, oral, nasal, and cecum mucosae at 1, 2, 3, 5, and 14 days after MOC aspiration (Figure 1A). Compared with PBS aspiration, MOC aspiration induced significant compositional changes (β diversity) in lung microbiota; however, these changes were time restricted, evident only at Days 1, 2 and 3 and not at Days 5 and 14 after MOC aspiration (Figure 1B). Correspondingly, taxonomic evaluation confirmed the presence of MOC taxa during the first 3 days after aspiration but not thereafter (Figure 1D). Measurement of the bacterial load after MOC aspiration is also supportive of rapid clearance of this microbes (Figure E2). In contrast to changes in the lung, no significant compositional changes (based on β diversity) were observed in the microbiota of the oral, nasal, and cecum mucosae after MOC aspiration (Figure 1C).

Increased Lower-Airway Inflammation after MOC
A transcriptomic approach was used to evaluate the lower-airway host immune response to MOC. RNA sequencing was performed on lung homogenates collected on Days 1 and 14 after a single MOC or PBS control aspiration. PCoA showed that, at both time points, lung transcriptomes from MOC versus PBS aspiration differed (Figure 2A). Accordingly, volcano plots identified 1,776 differentially regulated genes between murine groups (Figures E3A and E3B and Table E3). IPA showed that

MOC aspiration induced T cell–signaling pathways (including TLR signaling), Th1 pathways, Th17 activation pathways (including SAA1), inflammasome pathways, P38 MAPK pathways, and PI3K/AKT-signaling pathways (Figure 2D). A focused examination of the TLR signaling pathway identified upregulation of genes related to the MyD88-signaling pathway (Figures 2B and 2C).

We used FACS to monitor T-lymphocyte subpopulations over 14 days after MOC aspiration. This analysis revealed that MOC aspiration induced a transient inflammatory response characterized by an increase in *1*) CD4$^+$- and CD8$^+$-activated T cells, *2*) CD4$^+$- and CD8$^+$PD1$^+$-expressing cells, and *3*) regulatory T cells (Tregs) (Figure 3). At Day 14, there was a significant increase in CD4$^+$IFNγ^+- (Th1-like) and IL-17$^+$–producing T cells (both Th17 and $\gamma\delta$ T cells, Figures 3E–3G). Single-strain aspiration with *S. mitis*, *P. melaninogenica*, and *V. parvula* showed a greater proinflammatory response with *V. parvula* than with PBS (Figure E4).

Cytokine/chemokine expression (Luminex multiplex assay) was evaluated in lung homogenates at 14 days after aspiration (Figure 4A). Unsupervised clustering revealed almost distinct segregation by experimental condition, wherein MOC aspiration was associated with increased levels of IL-17 compared with PBS aspiration. Multispectral immunohistochemistry showed increased airway CD3$^+$, CD4$^+$, CD8$^+$, macrophages, and neutrophils after MOC aspiration compared with PBS aspiration (Figures 4C and 4D).

Inflammatory Profile after MOC Aspiration in MyD88-Deficient Mice
Next, to determine the contribution of the MyD88-dependent innate immune pathway to the lower-airway immune response induced in response to MOC aspiration, we evaluated the effect of MOC aspiration in MyD88KO mice. FACS T-cell profiling showed both baseline and MOC aspiration–induced differences in immune status within MyD88KO and wild-type mice (Figure 5). Compared with changes observed in wild-type mice, the following T-cell responses to MOC aspiration were blunted in MyD88KO mice: *1*) CD4$^+$PD1$^+$ T cells, *2*) IL-17–producing T cells (Th17 and $\gamma\delta$ T cells), and *3*) CD4$^+$FoxP3$^+$ T cells (Figure 5). Conversely, the CD4$^+$/IFNγ^+ T-cell immune response

to MOC aspiration was not blunted in MyD88KO mice. These data suggested that MyD88 signaling influences the induction of proinflammatory IL-17 but not Th1 cells after MOC aspiration.

IL-17–Driven Lung Inflammation Does Not Change the Composition of the Lung Microbiota
Cross-sectional human data have shown an association between enrichment of the lower-airway microbiota with oral commensals and the Th17 phenotype (12). It is not possible to determine the directionality of this association in cross-sectional human data. To determine whether the increased lung IL-17 inflammatory phenotype contributes to the microbial composition of the lower-airway microbiota, we evaluated the composition of the lower-airway microbiota in a mouse model with hyperactive STAT3 selectively expressed in T lymphocytes. We chose this experimental system because it is associated with a pronounced Th17 bias and IL-17–mediated inflammation in the lung (14). Compared with the lung microbiota of wild-type mice, the lung microbiota in STAT3 mutant mice did not show differences in α or β diversity (Figure E5), nor did they show differences in taxonomic composition (based on DESeq2 analysis, data not shown). Together, these findings support that the IL-17 inflammatory response elicited after MOC aspiration does not necessarily lead to a change in the lung-microbiota composition in otherwise healthy mice.

MOC Aspiration and Host Susceptibility to *S. pneumoniae*
To test our hypothesis that MOC aspiration influences host susceptibly to *S. pneumoniae*, we first examined *S. pneumoniae* recovery from the lung 24 hours after a low-dose *S. pneumoniae* challenge; challenges were conducted at different time points after MOC aspiration (Figure 6A). Concomitant MOC aspiration and *S. pneumoniae* challenge did not alter pathogen recovery. In contrast, compared with PBS control aspiration, MOC aspiration performed 1 day or 14 days before *S. pneumoniae* challenge resulted in a significant reduction in the recovery of *S. pneumoniae* from the lower airways (Figure 6B; $P < 0.05$). Furthermore, heat-killed MOC aspiration 14 days before *S. pneumoniae* challenge did not result in
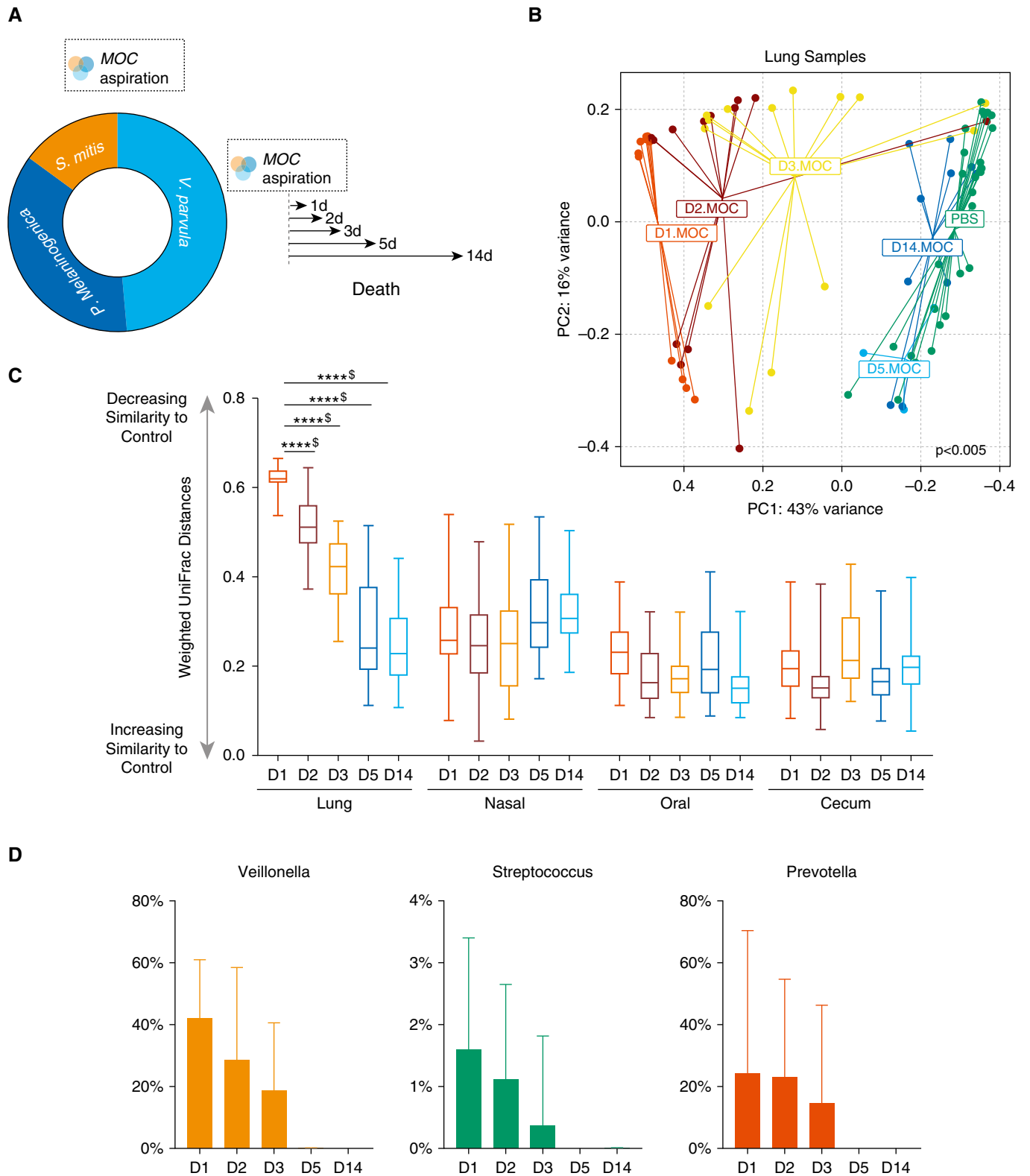
Figure 1. Lower-airway aspiration with human oral commensals leads to transient lower-airway dysbiosis. (*A*) Schematic experiment design of aspiration with a mixture of human oral commensals (MOC). Mice exposed to MOC challenge and subsequent killing on Day 1 (D1) (*n* = 12), D2 (*n* = 13), D3 (*n* = 14), D5 (*n* = 5), and D14 (*n* = 4) and mice exposed to phosphate-buffered saline (PBS) (*n* = 29). (*B*) PC analysis plot showing β diversity based on weighted unique fraction distance on lung samples. Differential clustering occurs early on after exposure to MOC versus PBS (permutational multivariate ANOVA *P* < 0.001). By D5, all of the samples exposed to MOC overlapped with PBS samples (PBS = dark green cluster, D5 = blue cluster, and D14 = light blue

a significant change in the recovery of S. pneumoniae from the lower airways as compared with PBS control aspiration (Figure E6).

We next evaluated survival after challenge with a sublethal median lethal dose or a 100% lethal dose (LD_{100}) of S. pneumoniae (Figure 6C). Concomitant aspiration of MOC and S. pneumoniae did not alter survival. However, compared with PBS aspiration, aspiration of MOC 14 days before sublethal S. pneumoniae challenge significantly improved survival (Figure 6D; 40% vs. 100%, Mantel-Cox Survival $P < 0.05$). Similarly, MOC aspiration 14 days before lethal LD_{100} S. pneumoniae challenge improved survival (Figure 6D; 0% vs. 100%, $P = 0.002$). Given the concern for possible cross-immunization between the S. mitis contained in MOC and S. pneumoniae (31), we then tested whether the beneficial effect of MOC was dependent on S. mitis. To this end, mice were aspirated with 1) PBS, 2) S. mitis, 3) V. parvula plus P. melaninogenica, or 4) MOC 14 days before S. pneumoniae challenge. This experiment shows that the beneficial effect of MOC aspiration on post–S. pneumoniae recovery and mortality was maintained despite the removal of S. mitis (Figure E7).

Discussion

In mice, a single aspiration event with oral commensals was cleared from the lung in less than 5 days but induced a Th17 inflammatory response and resistance to a respiratory pathogen (S. pneumoniae) that persisted for at least 14 days. These data support the counterintuitive idea that transient lower-airway dysbiosis from microaspiration with oral commensals has immunological benefits, protecting against a common respiratory pathogen.

Enrichment of the lower airways with oral commensals has been a common finding in many human studies using culture-independent methods. In healthy people, this microbial signature has been associated with an increase in the host immune inflammatory phenotype (3, 12). In case/control studies using subjects with different disease states, this microbial signature has been found with a higher prevalence in healthy subjects in some reports (32, 33), whereas it has been found with a higher prevalence in subjects with disease in other reports (4, 34–37). The bacterial load of the upper airway exceeds by many folds the load of the lower airways in most conditions, and given the continuous nature of the upper and lower respiratory tract, it is not surprising to see that oral commensals are commonly found in the lower airways. Imaging studies have documented microaspiration occurring commonly among healthy individuals (38). These data are in discordance with studies that demonstrated clear differences in the microbial composition of the upper and lower airways in lambs (39) and mice (40, 41). This has led to the suggestion that these differences are due to humans' bipedal and upright posture (42). However, a more fundamental question is whether this evolutionary difference of the microbial exposure in the respiratory tract has a protective or detrimental immunological role. To evaluate this experimentally, we modeled aspiration with human oral commensals in wild-type mice.

The host immune phenotype elicited by a single MOC aspiration in wild-type mice is consistent with observations seen in cross-sectional studies in human cohorts, in which enrichment of the lower-airway microbiota with oral commensals is associated with IL-17 inflammation (3, 12). The experimental conditions evaluated here support the hypothesis that significant lung immune changes follow transient dysbiosis of the lower-airway microbiota. As seen here in our MOC aspiration murine model, aspirated microbes are rapidly cleared by host defenses. MOC aspiration recruits neutrophils, Th1 cells, Th17 cells, and IL-17–producing T cells into the lower airway. Our experiments support that the increase in the lower-airway IL-17 inflammatory tone is a consequence of the exposure to oral commensals through microaspiration. The results of a single MOC aspiration provide a framework to understand the association between enrichment of the lower-airway microbiota with oral commensals and lung inflammatory tone in humans. In contrast, IL-17 inflammation did not lead to significant change in the microbial composition of the lower airways.

The increased inflammation induced by a MOC likely contributed to the reduced growth of S. pneumoniae seen beyond the duration of the transient lower-airway dysbiosis. Improved pathogen control through lower-airway immunological priming, combined with induction of counterregulatory phenomena manifested by increased Treg- and $PD1^+$-expressing T cells, likely contributes to the reduced mortality after S. pneumoniae challenge. The postaspiration inflammatory tone induced by a single MOC aspiration might therefore be beneficial by protecting the lung from pathogens and from sepsis. Alternatively, it is quite possible that repeated episodes of a transiently altered lung microbiome due to MOC aspiration lead to chronic inflammation and could predispose the lungs to structural damage and reduced lung function. The latter hypothesis was not evaluated in the current investigation, but it is important to note here that these two possibilities are not mutually exclusive.

Aspiration of a MOC constitutes a broad exposure to multiple molecules, including pathogen-associated molecular patterns that activate the innate immune response. Deficiency of MyD88 blunted the increase of the pulmonary IL-17–producing cells: Th17 and γδ T cells. These results are consistent with reports of innate immune activation leading to airway reactivity (13). MyD88 expression was also required for induction of counterregulatory Tregs and checkpoint-inhibited T cells but was not required for $CD4^+/CD8^+$ activation and Th1-cell induction. MyD88-independent induction pathways may include inflammasome-related pathways such as NOD2 (43) and TRIF (44), leading to a Th1 inflammatory response in the MyD88KO mice after MOC aspiration.

Figure 1. (Continued). cluster). (C) Dissimilarity between MOC aspiration versus PBS samples by mucosal surface (****$P < 0.0001$ and $^\$Q < 0.05$ for all comparisons). Box and whisker plots demonstrate median (interquartile range) with whiskers set at minimum to maximum. (D) Relative abundance levels of S., V., and P. by day, with significant clearance over time and disappearance by D5 ($P < 0.01$ for all comparisons). D1 = Day 1 after MOC aspiration; D2 = Day 2 after MOC aspiration; D3 = Day 3 after MOC aspiration; D5 = Day 5 after MOC aspiration; D14 = Day 14 after MOC aspiration; P. = Prevotella; PC = principal coordinate; S. = Streptococcus; V. = Veillonella.
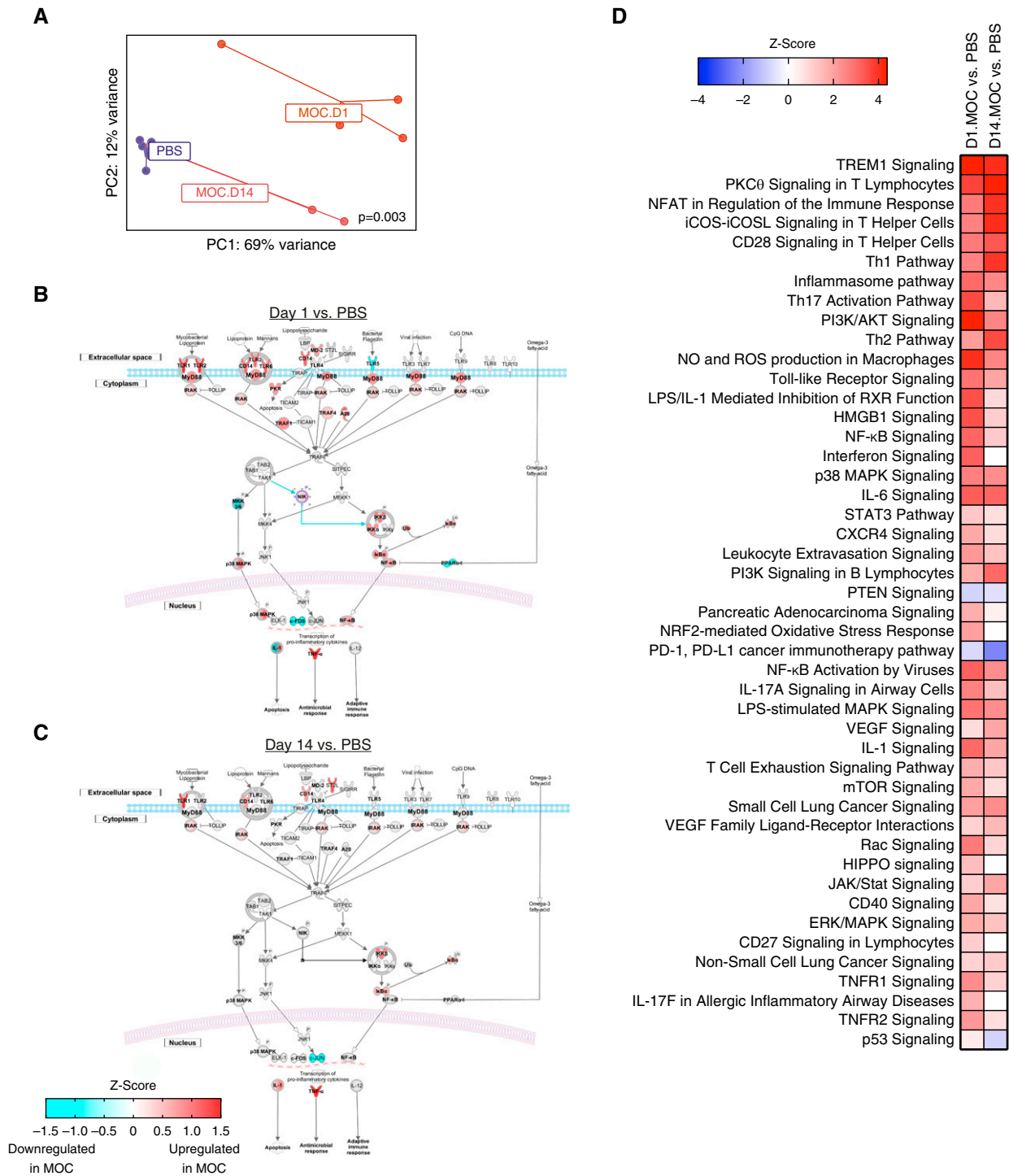
Figure 2. Differential gene expression demonstrates inflammation up to 14 days after aspiration with a mixture of human oral commensals (MOC). (*A*) PC analysis of gene expression based on the Bray-Curtis dissimilarity index (permutational multivariate ANOVA $P = 0.003$). (*B* and *C*) Ingenuity pathway analysis network analysis for transcriptomic changes after MOC aspiration on Day 1 (D1) and D14, respectively. (*D*) Ingenuity pathway analysis on differentially expressed genes between MOC versus PBS for D1 and D14 (false discovery rate < 0.1). NK = natural killer cell; P = phosphorylation/dephosphorylation; PBS = phosphate-buffered saline; PC = principal coordinate; ROS = reactive oxygen species; Th = T-helper cell; Ub = Ubiquitination.

The data presented here support that the immunological effects of a single MOC aspiration provide a beneficial effect on host pathogen susceptibility that is durable beyond the transient lower-airway dysbiosis induced by MOC aspiration. However, concerning the limitations of this study, we should state that all experiments were performed on female mice. Differences based on sex are expected (45, 46), and studies will need to be repeated with male mice. Another limitation is that we used
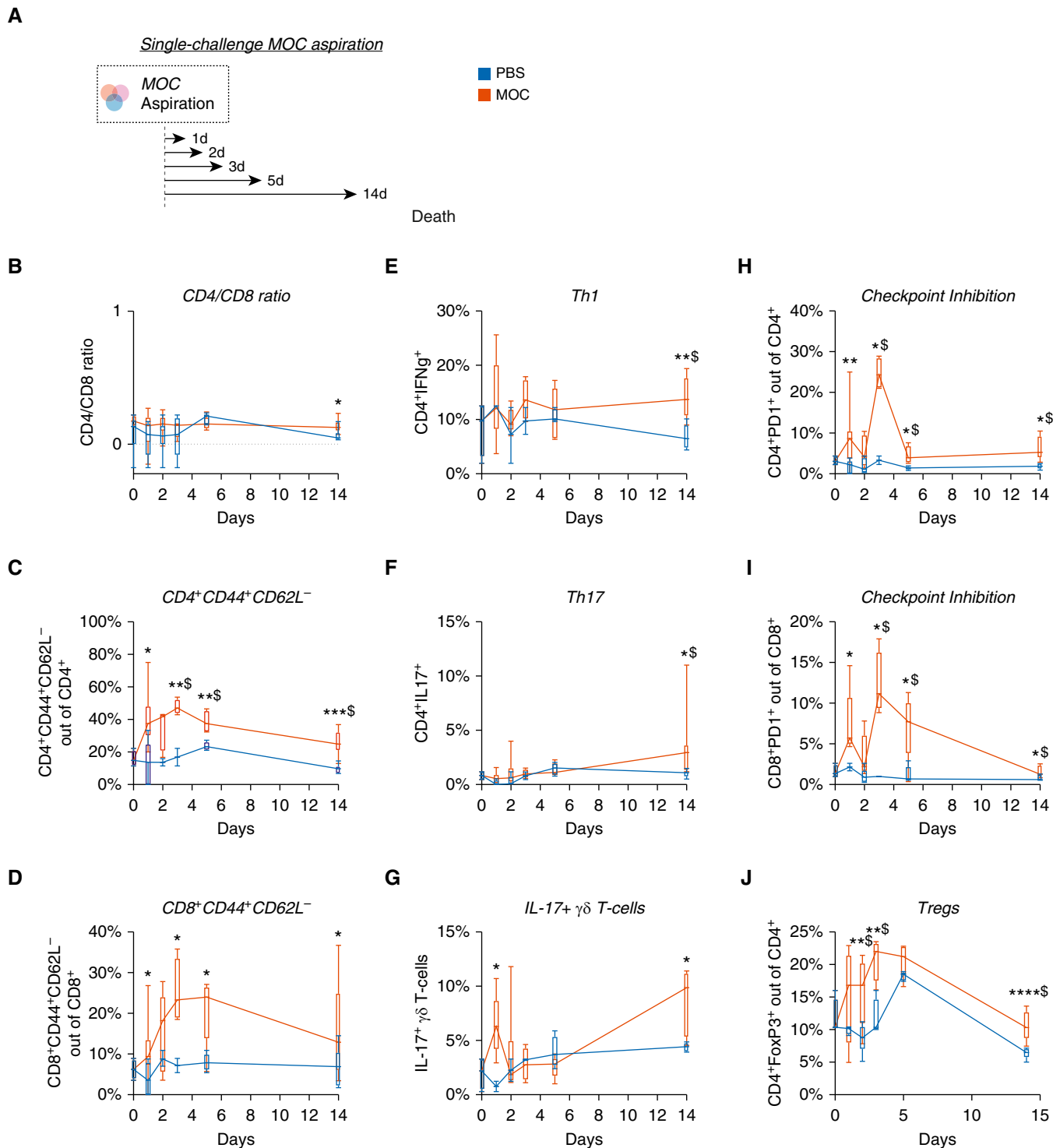
Figure 3. Lower-airway aspiration with oral commensals leads to a prolonged inflammatory response. (*A*) Schematic experimental design with killing on Days 1 (*n* = 5), 2 (*n* = 5), 3 (*n* = 5), 5 (*n* = 5), and 14 (*n* = 5). (*B–J*) Values for CD4/CD8 ratio, activation of T cells (CD4$^+$CD44$^+$CD62L$^-$ and CD8$^+$CD44$^+$CD62L$^-$), T-helper cell type 1 (Th1) cells, Th17 cells, IL-17$^+$ γδ T cells, checkpoint-inhibited T cells (CD4$^+$PD1$^+$ and CD8$^+$PD1$^+$), and Tregs over 14 days after MOC aspiration as compared with PBS control animals. *$P < 0.05$, **$P < 0.01$, ***$P < 0.001$, ****$P < 0.0001$, and $^\$Q < 0.05$. Box and whisker plots demonstrate median (interquartile range) with minimum to maximum values. MOC = mixture of human oral commensals; PBS = phosphate-buffered saline; Treg = regulatory T cell.
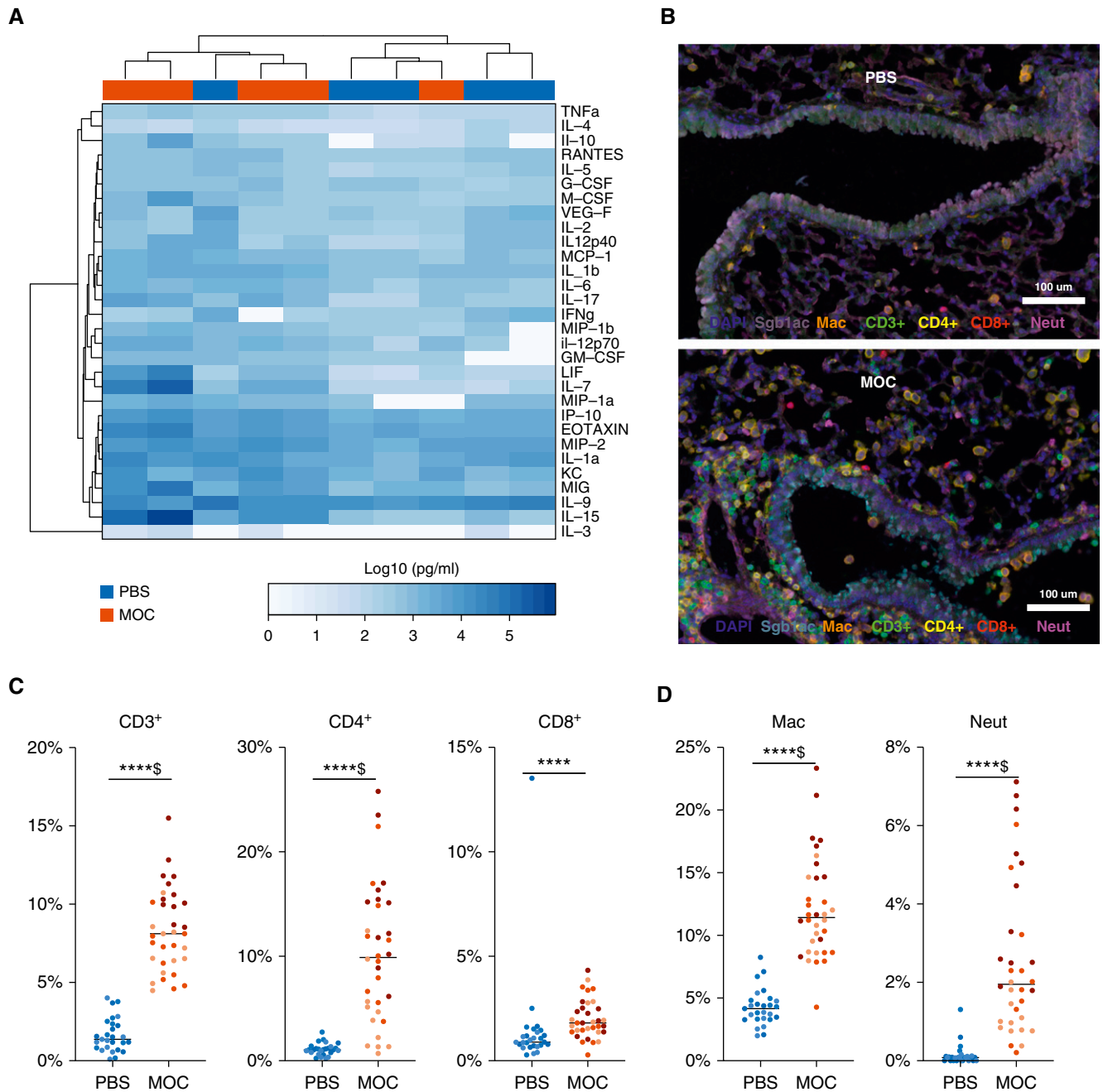
Figure 4. Histological changes after aspiration with a mixture of human oral commensals (MOC). (*A*) Heatmap for cytokine measurements on lung homogenates using Luminex with unsupervised hierarchical clustering (based on Bray-Curtis dissimilarity index). MOC aspiration was associated with greater levels of IL-17 ($P = 0.007$). (*B*) Histological evaluation on low-power multispectral immunohistochemistry from Vectral Imaging with immune histochemistry staining for Mac (F4/80), CD3$^+$, Neut (myeloperoxidase), club cells (CC10), CD4$^+$, and CD8$^+$ between MOC aspiration and phosphate-buffered saline (PBS) at Day 14. (*C*) Comparison of quantification of the cells per multispectral immunohistochemistry between MOC aspiration and PBS at Day 14. $N = 3$ for each condition; each dot represents different fields analyzed; lines represent the median value for each group. (*D*) Comparisons of macrophage and neutrophil percentages between MOC aspiration and PBS at Day 14. $N = 3$ for each condition; each dot represents different fields analyzed. ****$P < 0.0001$ and $^\$Q < 0.05$. Mac = macrophages; Neut = neutrophils.

human oral commensals to induce lower-airway dysbiosis, as these are the microbes found to be associated with inflammatory tone in the human lung. This MOC aspiration model is physiologically consistent with what is expected in human aspiration, in which a mixture of microbes, rather than a single bacterium, is aspirated in the lower airways. Further assessment of murine oral commensals, instead of human commensals, in the murine lower airway may also produce similar inflammation, but this was not assessed in this study. Furthermore, the relative contribution to each single bacterium (and/or potentiating
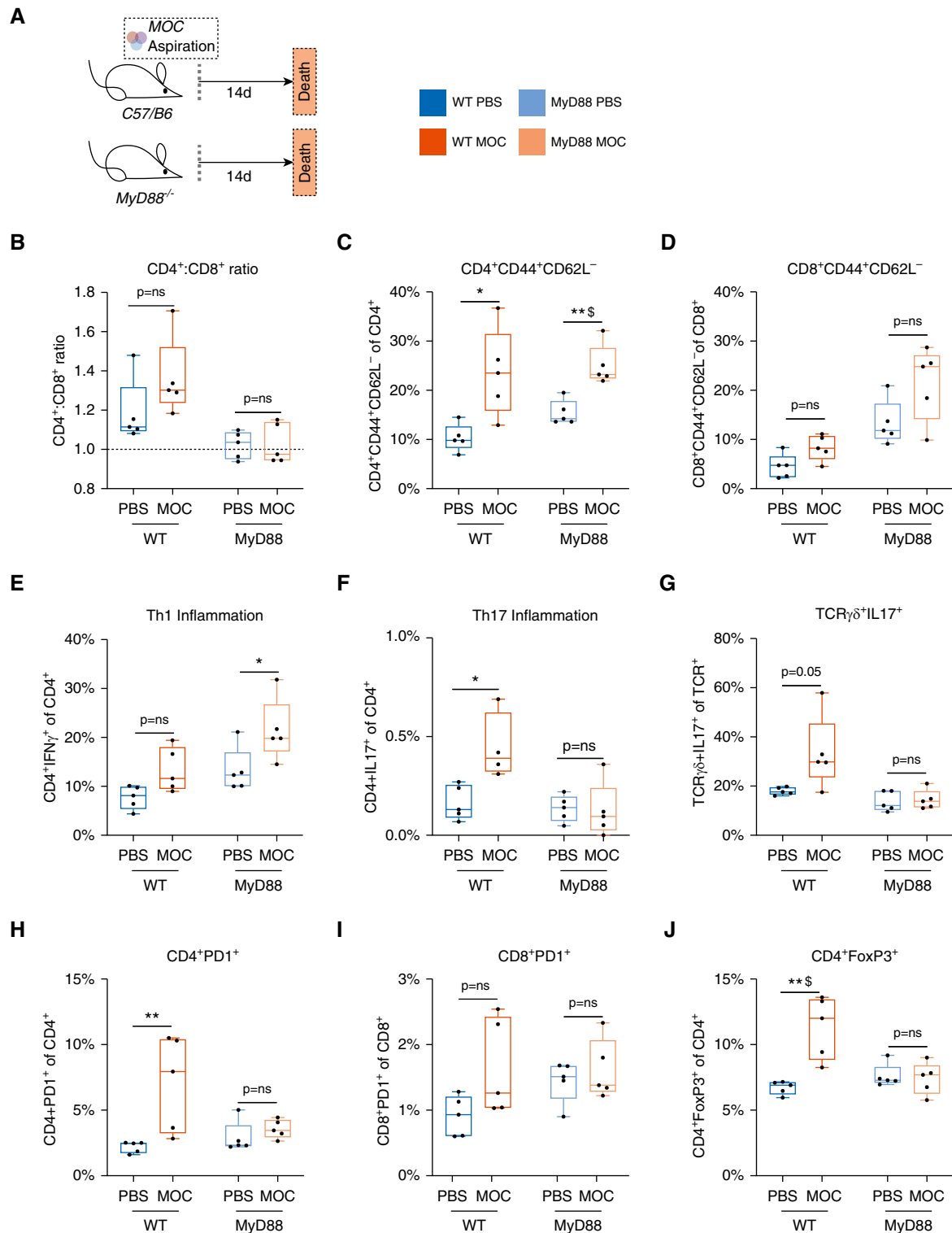
Figure 5. MyD88 adaptor protein is necessary for lung recruitment of IL-17 inflammation and markers of exhaustion but is not necessary for activation and T-helper cell type 1 (Th1) inflammation after aspiration with a mixture of human oral commensals (MOC). (*A*) Schematic experimental design with killing at Day 14 after MOC/phosphate-buffered saline (PBS) exposure in both WT (PBS *n* = 5, MOC *n* = 5) and MyD88KO (PBS *n* = 5, MOC *n* = 5) mice. (*B–J*) Values for CD4/CD8 ratio, activation T cells (CD4$^+$CD44$^+$CD62L$^-$ and CD8$^+$CD44$^+$CD62L$^-$), Th1 cells, Th17 cells, IL-17$^+$ γδ T cells, checkpoint-inhibited T cells (CD4$^+$PD1$^+$ and CD8$^+$PD1$^+$), and Tregs at 14 days after MOC aspiration as compared with PBS. *$P < 0.05$, **$P < 0.01$, and $^\$Q < 0.05$. Box and whisker plots demonstrate median (interquartile range) with minimum to maximum values. ns = not significant; TCR = T-cell receptor; Treg = regulatory T cell; WT = wild type.
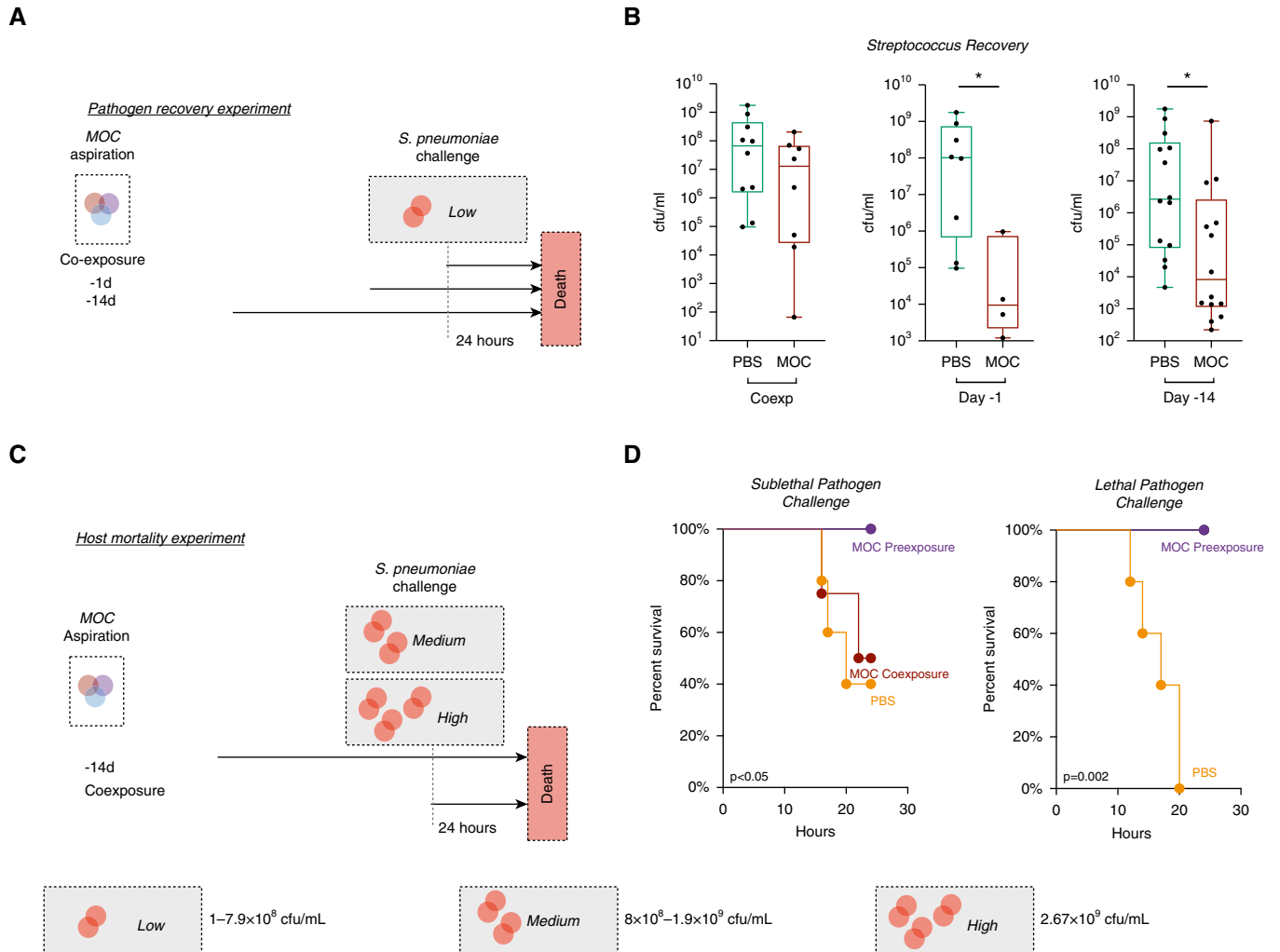
Figure 6. Modulation of host susceptibility to *Streptococcus pneumoniae* after aspiration with a mixture of human oral commensals (MOC). (*A*) Schematic of experiment with MOC exposure and pathogen challenge with low dose of *S. pneumoniae*. (*B*) Recovery of *S. pneumoniae* at 24 hours after pathogen challenge. Box and whisker plots demonstrate median (interquartile range) with minimum to maximum values. *$P < 0.05$. (*C*) Schematic of experiment with MOC exposure and pathogen challenge with a medium (6.5×10^8 cfu/ml) and high dose (2.67×10^9 cfu/ml) of *S. pneumoniae* (phosphate-buffered saline [PBS] $n = 5$, MOC coexposure $n = 5$, and MOC preexposure $n = 5$). (*D*) Survival curves of mice after pathogen challenge (*P* value based on Mantel-Cox; PBS $n = 5$, MOC preexposure $n = 5$). Coexp = coexposure.

effect of multiple different bacteria) to the host immune tone and susceptibility to pathogens will need to be explored further with different experimental approaches that will help dissect the molecular mechanisms driving the host immune response. In addition, in this study, we did not explore the longevity of the inflammatory response beyond 14 days. The results of this study might be seen as discordant with the clinical observation that subjects with frequent aspiration events suffer from frequent pneumonia with isolation of respiratory pathogens (47, 48). It is important to note that the effects of chronic aspiration were not assessed in this study and would be best modeled by repeated

episodes of MOC aspiration. It is possible that repetitive MOC aspiration events may lead to a very different host immune phenotype, shifting the balance of proinflammatory and counterregulatory inflammatory mechanisms, and may lead to T-cell exhaustion, resulting in a different host immune response to pathogens. Further immune profiling and survival over a longer term (>24 h) after pathogen challenge among MOC-aspirated mice may further help elucidate the immune mechanism involved. Finally, here we focus on the effects of MOC aspiration on the susceptibility to *S. pneumoniae* because this is the most common respiratory pathogen responsible for community-acquired

pneumonia. The role for MOC aspiration on hosts' susceptibility to other respiratory pathogens will need to be explored further.

In conclusion, the induction of transient lower-airway dysbiosis after aspiration with human oral commensals leads to a prolonged change in lower-airway inflammatory tone and the immune response to pathogens. The recruitment of IFN-γ– and IL-17–producing cells after aspiration with human oral anaerobes suggests that there is a physiological role for these commensal bacteria in the immunological priming in the lung mucosa, which is consistent with data on the oral (49) and gastrointestinal microbial host immune interphase (50–52); however,

in the lung, there are fundamental differences in the microbial colonization dynamics, and these microbes may therefore be present during a relatively short period of time after aspiration. The results described in the current investigation suggest that sporadic episodes of aspiration may represent an important physiological event. Further research must be performed to extend the observations made here, evaluating the effects of repetitive aspiration events and impairment of host immune response due to a secondary risk factors (e.g., cigarette smoke) to assess the relevance of dysbiosis with oral commensals in the chronic inflammatory processes affecting the lung. ■

Author disclosures are available with the text of this article at www.atsjournals.org.

References

1. Bassis CM, Erb-Downward JR, Dickson RP, Freeman CM, Schmidt TM, Young VB, et al. Analysis of the upper respiratory tract microbiotas as the source of the lung and gastric microbiotas in healthy individuals. *mBio* 2015;6:e00037.
2. Dickson RP, Erb-Downward JR, Freeman CM, McCloskey L, Falkowski NR, Huffnagle GB, et al. Bacterial topography of the healthy human lower respiratory tract. *mBio* 2017;8:e02287-16.
3. Segal LN, Alekseyenko AV, Clemente JC, Kulkarni R, Wu B, Gao Z, et al. Enrichment of lung microbiome with supraglottic taxa is associated with increased pulmonary inflammation. *Microbiome* 2013; 1:19. [Published erratum appears in *Microbiome* 2:21.]
4. Huang YJ, Nariya S, Harris JM, Lynch SV, Choy DF, Arron JR, et al. The airway microbiome in patients with severe asthma: associations with disease features and severity. *J Allergy Clin Immunol* 2015;136: 874–884.
5. Huang YJ, Nelson CE, Brodie EL, Desantis TZ, Baek MS, Liu J, et al.; NHLBI's Asthma Clinical Research Network. Airway microbiota and bronchial hyperresponsiveness in patients with suboptimally controlled asthma. *J Allergy Clin Immunol* 2011;127:372–381, e1–e3.
6. Bernasconi E, Pattaroni C, Koutsokera A, Pison C, Kessler R, Benden C, et al.; SysCLAD Consortium. Airway microbiota determines innate cell inflammatory or tissue remodeling profiles in lung transplantation. *Am J Respir Crit Care Med* 2016;194:1252–1263.
7. Erb-Downward JR, Thompson DL, Han MK, Freeman CM, McCloskey L, Schmidt LA, et al. Analysis of the lung microbiome in the "healthy" smoker and in COPD. *PLoS One* 2011;6:e16384.
8. Sze MA, Dimitriu PA, Suzuki M, McDonough JE, Campbell JD, Brothers JF, et al. Host response to the lung microbiome in chronic obstructive pulmonary disease. *Am J Respir Crit Care Med* 2015;192:438–445.
9. Sze MA, Hogg JC, Sin DD. Bacterial microbiome of lungs in COPD. *Int J Chron Obstruct Pulmon Dis* 2014;9:229–238.
10. Pragman AA, Kim HB, Reilly CS, Wendt C, Isaacson RE. The lung microbiome in moderate and severe chronic obstructive pulmonary disease. *PLoS One* 2012;7:e47305.
11. Pragman AA, Lyu T, Baller JA, Gould TJ, Kelly RF, Reilly CS, et al. The lung tissue microbiota of mild and moderate chronic obstructive pulmonary disease. *Microbiome* 2018;6:7.
12. Segal LN, Clemente JC, Tsay J-CJ, Koralov SB, Keller BC, Wu BG, et al. Enrichment of the lung microbiome with oral taxa is associated with lung inflammation of a Th17 phenotype. *Nat Microbiol* 2016;1: 16031.
13. Cai T, Qiu J, Ji Y, Li W, Ding Z, Suo C, et al. IL-17–producing ST2$^+$ group 2 innate lymphoid cells play a pathogenic role in lung inflammation. *J Allergy Clin Immunol* 2019;143:229–244, e9.
14. Fogli LK, Sundrud MS, Goel S, Bajwa S, Jensen K, Derudder E, et al. T cell–derived IL-17 mediates epithelial changes in the airway and drives pulmonary neutrophilia. *J Immunol* 2013;191: 3100–3111. [Published erratum appears in *J Immunol* 191: 5318.]
15. Segal LN, Clemente JC, Wu BG, Wikoff WR, Gao Z, Li Y, et al. Randomised, double-blind, placebo-controlled trial with azithromycin selects for anti-inflammatory microbial metabolites in the emphysematous lung. *Thorax* 2017;72:13–22.
16. Salter SJ, Cox MJ, Turek EM, Calus ST, Cookson WO, Moffatt MF, et al. Reagent and laboratory contamination can critically impact sequence-based microbiome analyses. *BMC Biol* 2014;12:87.

17. Walters WA, Caporaso JG, Lauber CL, Berg-Lyons D, Fierer N, Knight R. PrimerProspector: de novo design and taxonomic analysis of barcoded polymerase chain reaction primers. *Bioinformatics* 2011; 27:1159–1161.
18. Chaturvedi AK, Gaydos CA, Agreda P, Holden JP, Chatterjee N, Goedert JJ, et al. *Chlamydia pneumoniae* infection and risk for lung cancer. *Cancer Epidemiol Biomarkers Prev* 2010;19: 1498–1505.
19. Bolyen E, Rideout JR, Dillon MR, Bokulich NA, Abnet C, Al-Ghalith GA, et al. QIIME 2: reproducible, interactive, scalable, and extensible microbiome data science [preprint]. PeerJ; 2018 [accessed 2018 Dec 3]. Available from: https://peerj.com/preprints/27295/.
20. Bolyen E, Rideout JR, Dillon MR, Bokulich NA, Abnet CC, Al-Ghalith GA, et al. Reproducible, interactive, scalable and extensible microbiome data science using QIIME 2. *Nat Biotechnol* 2019;37: 852–857.
21. Callahan BJ, McMurdie PJ, Rosen MJ, Han AW, Johnson AJ, Holmes SP. DADA2: high-resolution sample inference from Illumina amplicon data. *Nat Methods* 2016;13:581–583.
22. Lozupone C, Knight R. UniFrac: a new phylogenetic method for comparing microbial communities. *Appl Environ Microbiol* 2005;71: 8228–8235.
23. Dray S, Dufour A-B. The ade4 package: implementing the duality diagram for ecologists. *J Stat Softw* 2007;22:1–20.
24. Dobin A, Davis CA, Schlesinger F, Drenkow J, Zaleski C, Jha S, et al. STAR: ultrafast universal RNA-seq aligner. *Bioinformatics* 2013;29: 15–21.
25. Liao Y, Smyth GK, Shi W. The Subread aligner: fast, accurate and scalable read mapping by seed-and-vote. *Nucleic Acids Res* 2013; 41:e108.
26. Liao Y, Smyth GK, Shi W. featureCounts: an efficient general purpose program for assigning sequence reads to genomic features. *Bioinformatics* 2014;30:923–930.
27. Love MI, Huber W, Anders S. Moderated estimation of fold change and dispersion for RNA-seq data with DESeq2. *Genome Biol* 2014;15: 550.
28. Calvano SE, Xiao W, Richards DR, Felciano RM, Baker HV, Cho RJ, et al.; Inflamm and Host Response to Injury Large Scale Collab. Res. Program. A network-based analysis of systemic inflammation in humans. *Nature* 2005;437:1032–1037. [Published erratum appears in *Nature* 438:696.]
29. Krämer A, Green J, Pollard J Jr, Tugendreich S. Causal analysis approaches in ingenuity pathway analysis. *Bioinformatics* 2014;30: 523–530.
30. Reiner A, Yekutieli D, Benjamini Y. Identifying differentially expressed genes using false discovery rate controlling procedures. *Bioinformatics* 2003;19:368–375.
31. Shekhar S, Khan R, Schenck K, Petersen FC. Intranasal immunization with the commensal *Streptococcus mitis* confers protective immunity against pneumococcal lung infection. *Appl Environ Microbiol* 2019;85:e02235-18.
32. Sze MA, Dimitriu PA, Hayashi S, Elliott WM, McDonough JE, Gosselink JV, et al. The lung tissue microbiome in chronic obstructive pulmonary disease. *Am J Respir Crit Care Med* 2012; 185:1073–1080.
33. Pattaroni C, Watzenboeck ML, Schneidegger S, Kieser S, Wong NC, Bernasconi E, et al. Early-life formation of the microbial and immunological environment of the human airways. *Cell Host Microbe* 2018;24:857–865, e4.

34. Twigg HL III, Knox KS, Zhou J, Crothers KA, Nelson DE, Toh E, *et al*. Effect of advanced HIV infection on the respiratory microbiome. *Am J Respir Crit Care Med* 2016;194:226–235.

35. Tsay JJ, Wu BG, Badri MH, Clemente JC, Shen N, Meyn P, *et al*. Airway microbiota is associated with upregulation of the PI3K pathway in lung cancer. *Am J Respir Crit Care Med* 2018;198: 1188–1198.

36. Ren L, Zhang R, Rao J, Xiao Y, Zhang Z, Yang B, *et al*. Transcriptionally active lung microbiome and its association with bacterial biomass and host inflammatory status. *mSystems* 2018;3: e00199-18.

37. Yang D, Chen X, Wang J, Lou Q, Lou Y, Li L, *et al*. Dysregulated lung commensal bacteria drive interleukin-17B production to promote pulmonary fibrosis through their outer membrane vesicles. *Immunity* 2019;50:692–706, e7.

38. Gleeson K, Eggli DF, Maxwell SL. Quantitative aspiration during sleep in normal subjects. *Chest* 1997;111:1266–1272.

39. Glendinning L, Collie D, Wright S, Rutherford KMD, McLachlan G. Comparing microbiotas in the upper aerodigestive and lower respiratory tracts of lambs. *Microbiome* 2017;5: 145.

40. Barfod KK, Roggenbuck M, Hansen LH, Schjørring S, Larsen ST, Sørensen SJ, *et al*. The murine lung microbiome in relation to the intestinal and vaginal bacterial communities. *BMC Microbiol* 2013;13: 303.

41. Dickson RP, Erb-Downward JR, Falkowski NR, Hunter EM, Ashley SL, Huffnagle GB. The lung microbiota of healthy mice are highly variable, cluster by environment, and reflect variation in baseline lung innate immunity. *Am J Respir Crit Care Med* 2018;198: 497–508.

42. McGinniss JE, Collman RG. Of mice and men . . . and microbes: conclusions and cautions from a murine study of the lung microbiome and microbiome-immune interactions. *Am J Respir Crit Care Med* 2018;198:419–422.

43. Shaw MH, Reimer T, Sánchez-Valdepeñas C, Warner N, Kim YG, Fresno M, *et al*. T cell-intrinsic role of Nod2 in promoting type 1 immunity to *Toxoplasma gondii*. *Nat Immunol* 2009;10: 1267–1274.

44. Zhang Y, Jones M, McCabe A, Winslow GM, Avram D, MacNamara KC. MyD88 signaling in CD4 T cells promotes IFN-γ production and hematopoietic progenitor cell expansion in response to intracellular bacterial infection. *J Immunol* 2013;190:4725–4735.

45. Surcel M, Constantin C, Caruntu C, Zurac S, Neagu M. Inflammatory cytokine pattern is sex-dependent in mouse cutaneous melanoma experimental model. *J Immunol Res* 2017;2017:9212134.

46. Kay E, Gomez-Garcia L, Woodfin A, Scotland RS, Whiteford JR. Sexual dimorphisms in leukocyte trafficking in a mouse peritonitis model. *J Leukoc Biol* 2015;98:805–817.

47. Schmidt J, Holas M, Halvorson K, Reding M. Videofluoroscopic evidence of aspiration predicts pneumonia and death but not dehydration following stroke. *Dysphagia* 1994;9:7–11.

48. Croghan JE, Burke EM, Caplan S, Denman S. Pilot study of 12-month outcomes of nursing home patients with aspiration on videofluoroscopy. *Dysphagia* 1994;9:141–146.

49. Dutzan N, Abusleme L, Bridgeman H, Greenwell-Wild T, Zangerle-Murray T, Fife ME, *et al*. On-going mechanical damage from mastication drives homeostatic Th17 cell responses at the oral barrier. *Immunity* 2017;46:133–147.

50. Atarashi K, Tanoue T, Shima T, Imaoka A, Kuwahara T, Momose Y, *et al*. Induction of colonic regulatory T cells by indigenous *Clostridium* species. *Science* 2011;331:337–341.

51. Goto Y, Panea C, Nakato G, Cebula A, Lee C, Diez MG, *et al*. Segmented filamentous bacteria antigens presented by intestinal dendritic cells drive mucosal Th17 cell differentiation. *Immunity* 2014;40:594–607.

52. Ivanov II, Atarashi K, Manel N, Brodie EL, Shima T, Karaoz U, *et al*. Induction of intestinal Th17 cells by segmented filamentous bacteria. *Cell* 2009;139:485–498.